AGU PUBLICATIONS

JGR

Journal of Geophysical Research: Planets

RESEARCH ARTICLE
10.1002/2016JE005054

Key Points:
- Conditions for magnetization at Mercury are unique among terrestrial planets
- Temperature, chemistry, and field strength limit possible remanence carriers
- Further characterization of candidate minerals is needed to understand Mercury's crustal fields

Correspondence to:
B. E. Strauss,
strau204@umn.edu

Citation:
Strauss, B. E., J. M. Feinberg, and C. L. Johnson (2016), Magnetic mineralogy of the Mercurian lithosphere, *J. Geophys. Res. Planets*, *121*, 2225–2238, doi:10.1002/2016JE005054.

Received 11 APR 2016
Accepted 25 SEP 2016
Accepted article online 29 SEP 2016
Published online 11 NOV 2016

Magnetic mineralogy of the Mercurian lithosphere

B. E. Strauss[1], J. M. Feinberg[1], and C. L. Johnson[2,3]

[1]Institute for Rock Magnetism, Department of Earth Sciences, University of Minnesota, Twin Cities, Minneapolis, Minnesota, USA, [2]Department of Earth, Ocean and Atmospheric Sciences, University of British Columbia, Vancouver, British Columbia, Canada, [3]Planetary Science Institute, Tucson, Arizona, USA

Abstract Mercury and Earth are the only inner solar system planets with active, internally generated dynamo magnetic fields. The MErcury Surface, Space ENvironment, GEochemistry, and Ranging (MESSENGER) mission recently detected magnetic fields on Mercury that are consistent with lithospheric magnetization. We investigate the physical and chemical environment of Mercury's lithosphere, past and present, to establish the conditions under which magnetization may have been acquired and modified. Three factors are particularly crucial to the determination of crustal composition and iron mineralogy: redox conditions in the planet's crust and mantle, the iron content of the lithosphere, and, for any remanent magnetization, the temperature profile of the lithosphere and its evolution over time. We explore potential mechanisms for remanence acquisition and alteration on Mercury, whose surface environment is both hot and highly reducing. The long-term thermal history of Mercury's crust plays an important role in the longevity of any remanent crustal magnetization, which may be subject to remagnetization through thermal, viscous, and shock mechanisms. This thermal and compositional framework is used both to constrain plausible candidate minerals that could carry magnetic remanence on Mercury and to evaluate their capacity to acquire and retain sufficient magnetization to be detectable from satellite orbit. We propose that iron metal and its alloys are likely to be the dominant contributors to induced and remanent magnetization in Mercury's lithosphere, with additional contributions from iron silicides, sulfides, and carbides.

1. Introduction

Mercury and Earth are the only inner solar system planets with active, internally generated dynamo magnetic fields [*Ness et al.*, 1974; *Anderson et al.*, 2008, 2011; *Hulot et al.*, 2015]. The Earth's dynamo field has an average equatorial intensity of ~30 μT at the planet's surface and is dominantly dipolar, with secondary nondipole contributions existing on historical [*Jackson et al.*, 2000], archaeological [*Korte et al.*, 2011], and geological [*Aubert et al.*, 2010] timescales. In contrast, Mars and the Moon do not have present-day dynamo fields, although magnetized crustal rocks on Mars provide evidence for a strong field billions of years in the past [*Acuña et al.*, 1999; *Dunlop and Arkani-Hamed*, 2005], and there is mounting evidence for an early dynamo field on the Moon [*Fuller*, 1998; *Wieczorek et al.*, 2012; *Weiss and Tikoo*, 2014]. The dynamo history of Venus is unknown, in part because the resurfacing history of the planet may have erased any evidence for past core fields [e.g., *Schubert et al.*, 2005].

The present-day magnetic field of Mercury has been analyzed by magnetometers on Mariner 10 and the MErcury Surface, Space ENvironment, GEochemistry, and Ranging (MESSENGER) orbiter. These missions found an approximately dipolar field with an average moment of 190 nT R_M^3, where R_M = Mercury's radius [*Anderson et al.*, 2008, 2011; *Alexeev et al.*, 2010; *Johnson et al.*, 2012; *Philpott et al.*, 2014], equivalent to a surface field strength less than 1% of that of the Earth. The equator of Mercury's magnetic field is offset northward from the planet's geographical equator by ~480 km, and unlike Earth's field, Mercury's field is highly axisymmetric about the planet's rotational axis [*Anderson et al.*, 2011; *Johnson et al.*, 2012].

The Earth, the Moon, Mars, and most recently Mercury [*Johnson et al.*, 2015] all show evidence for crustal magnetization. Remanent magnetization, the ancient magnetization held by geological materials, is of particular importance for understanding planetary interiors because it can provide information about the intensity, orientation, and temporal variations of ancient dynamo fields, which in turn constrain models for the thermal evolution of a given planet or moon. Further, lithospheric magnetization, whether induced in a modern field or acquired in an ancient field and retained, yields indirect information about the distribution of iron-bearing

minerals. However, the interpretation of crustal magnetic fields on extraterrestrial bodies presents a series of challenges due to the limited types and amount of data available. In the optimal case, direct samples (e.g., rocks collected *in situ* on Earth and the Moon) may be analyzed to establish magnetic mineralogy and recording properties as well as radioisotopic ages for known source regions, enabling the interpretation of magnetizations. Indirect samples (e.g., meteorites) are also useful for the characterization of host bodies, but their records of magnetic fields are less straightforward to decipher because of the complex processes involved in delivering material from its host body to Earth and the lack of information regarding its exact provenance. Remote satellite observations detect the spatial distribution and intensity of magnetic fields that result from crustal magnetization, providing an alternate data set.

The intensity of magnetization that may be held by a given material is dependent on both the strength of the magnetizing field and the fundamental magnetic properties of the material, which are determined primarily by its composition and mineralogy. The interpretation of magnetization data collected by satellites is complicated by ambiguities surrounding the mechanisms and timing of remanence acquisition, the mineralogical properties of the recording material, and the physical and chemical conditions this material has been subject to since the time of initial remanence acquisition.

The first identifications of Mercury's crustal field [*Johnson et al.*, 2015] have been confirmed by spatially extensive low-altitude observations that cover much of the Northern Hemisphere [*Johnson et al.*, 2016]. Lithospheric fields are weak, typically < 30 nT at spacecraft altitudes, and the shortest anomaly wavelengths observed are a few tens of kilometers, even at spacecraft altitudes less than 10 km. The strongest measured fields are associated with the Caloris and circum-Caloris region including regions of smooth plains whose origin (volcanic or impact) is debated [*Denevi et al.*, 2013; *Hood*, 2015; *Johnson et al.*, 2016]. Elsewhere, field amplitudes are weaker and exhibit shorter coherence length scales, including over Mercury's northern volcanic plains [*Head et al.*, 2011]. Magnetic signatures are often, but not always, associated with impact basin interiors and/or ejecta materials [*Johnson et al.*, 2015, 2016]. Calculations show that in the absence of remanent magnetization, induced magnetization alone would require magnetized layer thicknesses in excess of 100 km [*Johnson et al.*, 2016] to explain the strongest crustal signals measured. Thus, although contributions from induced magnetization or viscous remanent magnetization (VRM) are possible, the MESSENGER data suggest a component of remanent magnetization acquired in an ancient field with a strength between that of Mercury's present dipole field and higher Earth-like values [*Johnson et al.*, 2015]. Studies of the chronology of acquisition of magnetization are still in progress but are not simple to elucidate. First, for remanent magnetization, timing is not obvious. For example, the strong magnetizations associated with the smooth plains in and around the Caloris Basin could be (1) as old as Caloris, (2) the age of the smooth plains, or (3) younger than the smooth plains if substantial intrusion followed the last episode of extrusive volcanism (~3.5 Ga) [*Byrne et al.*, 2016]. Unlike on Mars, magnetic signatures associated with craters show no obvious pattern with relative crater ages [*Johnson et al.*, 2016]. Second, determination of the respective roles of different mechanisms of magnetization on Mercury will require constraints on its magnetic mineralogy.

The interpretation of Mercury's crustal field is particularly challenging because of the limited information available regarding the physical and chemical environment of the planet's lithosphere. Here we describe constraints on that environment, past and present, in order to establish the conditions in which magnetization may have been acquired by crustal rocks. Three factors are central to the determination of Mercury's magnetic mineralogy: the temperature profile of the lithosphere and its evolution over time, redox conditions in the planet's crust and mantle, and the iron content of the lithosphere. We also explore possible mechanisms for remanence acquisition and alteration on Mercury and ultimately propose a suite of minerals that could be acting as carriers of the remanence responsible for measured magnetic anomalies.

2. Chemical and Thermal Constraints on Magnetization

Compared to other inner solar system planets, Mercury is both hot and highly reducing; thus, two of the primary controls on recorders of magnetism are thermodynamic stability conditions and, for remanent magnetization, the temperature profile of the lithosphere and its evolution over time. Here we describe the present-day redox conditions of the crust and summarize known constraints on the iron content of the crust and mantle. In addition, we outline the present-day thermal conditions of Mercury's crust and establish how these conditions may have varied over time.

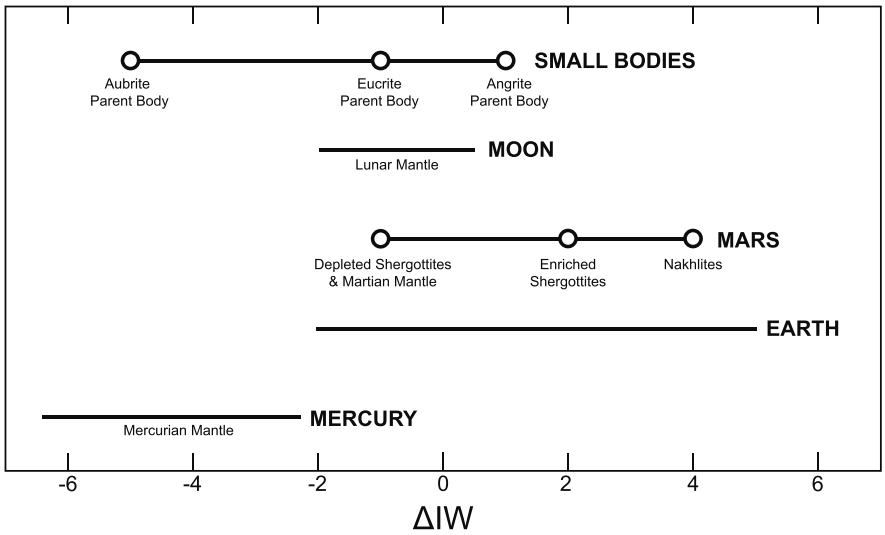

Figure 1. Summary of the redox conditions on small bodies, the Moon, and terrestrial planets. Redox conditions are shown relative to the iron-wüstite buffer (ΔIW). Modified from *Wadhwa* [2008] (via *Frost and McCammon* [2008] and *McCubbin et al.* [2012]).

2.1. Compositional Constraints

The chemistry of Mercury is unique among inner solar system planets. Mercury is highly reducing (Figure 1), with a reported mantle oxygen fugacity (f_{O_2}) in the range of −6.3 to −2.6ΔIW (log units below the iron-wüstite buffer) [*McCubbin et al.*, 2012], lower than those of most known small bodies and all other terrestrial planets [*Wadhwa*, 2008]. These estimates are based on the high sulfur and low iron oxide abundances measured at the planet's surface by MESSENGER's X-Ray Spectrometer (XRS) and Gamma-Ray Spectrometer, as well as Mercury's high average density [*Malavergne et al.*, 2010; *McCubbin et al.*, 2012]. This suggests that the carriers of remanence at Mercury will be markedly different from the iron oxide minerals that dominate relatively oxidizing systems like the Earth and Mars, as these minerals would be thermodynamically unstable in such reducing conditions.

The Earth's crust has an iron abundance of 5.6 wt % Fe [*Pepperhoff and Acet*, 2001; *Haynes et al.*, 2016], while the Martian crust has a high iron abundance of ∼20 wt % Fe [*Kletetschka et al.*, 2000] with an expected magnetic mineral content of 4–7% [*Dunlop and Arkani-Hamed*, 2005]. The combination of spectral data from MESSENGER with equilibrium crystallization modeling has been used to suggest an iron abundance of ≤ 10 wt % FeO (∼7.7 wt % Fe) [*Riner et al.*, 2010] in the crust of Mercury. Further constraints are provided by XRS measurements, which give ranges of 1.5–2 wt % Fe, indicating that Mercury is iron poor relative to Earth and Mars, but comparable to some lunar rocks [*Weider et al.*, 2012]. This low iron abundance, however, is still greater than that of melts from enstatite chondrites suggested as possible precursor materials for Mercury [*Weider et al.*, 2012, 2014].

Iron oxide minerals like those responsible for most remanent magnetization on Earth and Mars are therefore unlikely to form in the reducing crust of Mercury. Instead, most crustal iron is expected to be incorporated into other minerals whose thermodynamic stability conditions are more consistent with those of Mercury, particularly minerals whose occurrence and microtextures are controlled by igneous processes. The role of iron abundance should be considered with care, as low bulk crustal iron does not necessarily indicate that the population of materials responsible for remanence is dominated by iron-poor minerals. For instance, on the Earth's moon, where iron abundance ranges from Mercury-like values in the highlands to higher-than-Earth values in exposed lower crustal material [*Lucey et al.*, 1995], the magnetic mineralogy of crustal rocks is dominated by iron and iron-nickel phases, including kamacite (α-Fe), taenite (γ-Fe), and martensite (α_2-Fe) [*Fuller*, 1998; *Tikoo et al.*, 2012, 2014]. Some lunar breccias host fine-grained Fe-Ni alloys, while mare basalts are dominated by multidomain (MD) iron, with small amounts of single domain (SD) iron whose fine grain size and high shape anisotropy give rise to high coercivities of remanence [*Fuller*, 1998; *Tikoo et al.*, 2012].

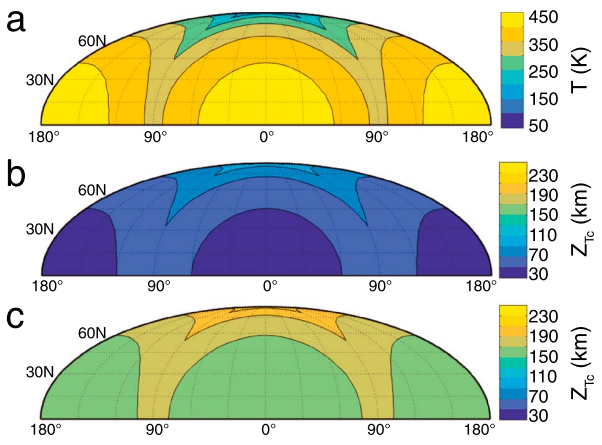

Figure 2. Temperature conditions at Mercury for present-day eccentricity (e = 0.2056) and heat flow. All temperatures in Kelvin; all depths in kilometer. (a) Average daily temperature at 1 m depth (beneath the depth of the penetration of the diurnal temperature wave). (b) Depth to the Curie temperature (Z_{Tc}) for pyrrhotite. (c) Z_{Tc} for iron.

2.2. Thermal Constraints

Temperature controls the fundamental rock magnetic properties of magnetic materials and, in turn, their ability to retain a permanent magnetization, though its effects vary with composition. Each ferromagnetic material has an intrinsic Curie temperature (T_C), above which its behavior is paramagnetic, with no long-range magnetic order, regardless of preexisting magnetic remanence. A thermoremanent magnetization (TRM) is acquired by a population of magnetic grains when they are cooled through their T_C in the presence of a magnetic field, causing a statistical alignment of their individual magnetizations, such that their net moment corresponds with the field's orientation and intensity. Conversely, if such grains are cooled through T_C in the absence of a field, magnetic moments of individuals grains do not align, and the resulting net moment is near zero.

The surface of Mercury experiences dramatic variations in temperature, due to its eccentric orbit (eccentricity, e = 0.2056) and 3:2 spin-orbit resonance, which together yield a daily insolation signature that varies with both latitude and longitude. The highest calculated noontime temperature under present-day orbital conditions is ~430°C (703 K) [*Vasavada et al.*, 1999], though the relevant boundary condition for thermoremanent magnetization acquisition and stability is the average daily surface temperature (T_S) at ~1 m depth in the crust (below the penetration depth of diurnal and seasonal temperature fluctuations in a regolith layer with low thermal conductivity) [*Vasavada et al.*, 1999]. As shown in Figure 2a, this ranges from −181°C (92 K) at the north and south poles (the spin poles) to 55°C (328 K) at the equator at 90°/270°E (the "cold" poles) and as high as 160°C (433 K) at the equator at 0°/180°E (the "hot" poles).

For a given average thermal gradient through the lithosphere, geographical variations in surface temperature translate directly into variations in the depth to a particular isotherm: the minimum (intermediate, maximum) depth occurs at the hot (cold, spin) poles. These variations, together with the thermal gradient in the lithosphere, are crucial determinants in the distribution of any crustal remanence. If the T_C of a magnetic mineral is less than the temperature in the crust at a given location and depth, the mineral will not be capable of retaining a TRM. Thermal evolution models for Mercury suggest an average present-day thermal gradient of ~4 K/km [*Williams et al.*, 2007; *Grott et al.*, 2011; *Tosi et al.*, 2013]. Figures 2b and 2c show the maximum possible thickness of the magnetized layer, or the depth to the T_C isotherm, for pyrrhotite (Fe_7S_8, T_C = 320–325°C) and iron (T_C = 770°C), respectively, in these thermal conditions. (Here we assume a homogeneous magnetic layer. Heterogeneous magnetic layers are outside the scope of this study, given the few constraints on Mercury's detailed crustal structure.) For iron, the maximum depth to T_C exceeds the average thickness of Mercury's crust (~40 km) [*James et al.*, 2014; *Padovan et al.*, 2015] over the entire planet, indicating that considering present-day thermal constraints alone, some magnetic minerals could hold a TRM in the upper mantle.

Neither orbital eccentricity nor planetary heat flux has been constant over geologic timescales. Mercury's orbital eccentricity may have ranged from e = ~0.12 to 0.31 over the last 50 Ma and from e = 0 to 0.4 over the past 4 Ga [*Correia and Laskar*, 2009]. Changes in e are expected to have occurred on much shorter timescales than changes in the spin-orbit resonance and thus to have been the primary control on surface temperature over time [*Correia and Laskar*, 2009]. Because the evolution of eccentricity is unknown, this effect cannot be assessed directly. Instead, bounds on T_S at a given location can be obtained by comparing the T_S values predicted at that location for a range of eccentricities. Figure 3a shows the maximum value of T_S as a function

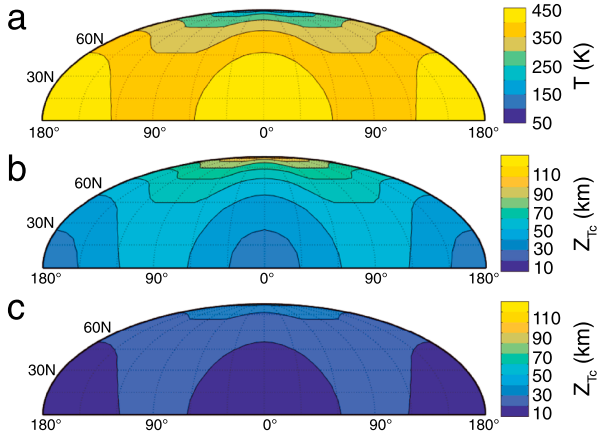

Figure 3. Maximum average daily temperature at Mercury for eccentricities ranging from $e = 0$ to 0.4. All temperatures in Kelvin; all depths in kilometer. (a) Maximum average daily temperature at 1 m depth. (b) Minimum depth to the Curie temperature (Z_{Tc}) for pyrrhotite for the temperature distribution in Figure 3a and a thermal gradient of 4 K/km (present day and recent geological past). (c) Z_{Tc} for pyrrhotite for the temperature distribution in Figure 3a and an ancient (~3–4 Ga) thermal gradient of 10 K/km. $Z_{Tc}(X)$ for a magnetic mineral X with Curie temperature $T_C(X)$ can be computed from that for pyrrhotite at a given thermal gradient, dT/dZ, by: $Z_{Tc}(X) = Z_{Tc}(\text{Pyrrhotite}) + ((T_C(X) - T_C(\text{Pyrrhotite}))/(dT/dZ))$.

of position computed for eccentricities ranging from 0 to 0.4. This provides an estimate of the upper bound on T_S at a particular location on Mercury over the past 4 Ga.

Thermal evolution models suggest that globally averaged thermal gradients at ~4 Ga were up to 2.5 times greater than those today [*Williams et al.*, 2007; *Grott et al.*, 2011; *Tosi et al.*, 2013]. The corresponding depth to T_C for a given magnetic mineral in the past can be obtained by scaling the values in present-day models by the ratio of the past to the present thermal gradient, as demonstrated for pyrrhotite in Figures 3b and 3c.

3. Magnetization and Demagnetization of the Magnetic Layer

The mechanisms of remanence acquisition and alteration in the magnetic layer of Mercury's crust are expected to be broadly similar to those at work on other terrestrial planets, particularly the Earth and its moon.

3.1. Acquisition of Primary Remanence

Magnetic minerals in a planet's crust can acquire a primary remanence during their formation or emplacement. The initial acquisition of remanence is controlled by the intensity of the applied field and the susceptibility of a given mineral to magnetization and limited by the mineral's saturation magnetization (M_s). As described in section 2.2, thermoremanent magnetization is produced when a population of ferromagnetic grains cools through the grains' T_C in the presence of the planetary magnetic field. Alternatively, minerals that precipitate in the presence of the planetary field and grow through a critical grain size, while remaining below their T_C can record the field as a chemical remanent magnetization (CRM). In some meteoritic iron-nickel alloys, grain growth, partitioning, and chemical changes continue during cooling below the high Curie temperatures of individual minerals, but above the lower temperature martensitic phase transformation. The resulting remanence is not a simple TRM or CRM and may instead be considered a thermochemical remanent magnetization.

The theoretical maximum crustal magnetic field intensity in a given region scales with the volume of the magnetized material (i.e., the thickness of the magnetic layer) and is controlled by variations in M_s between materials. In the same applied field, a thin layer of a mineral with high M_s can account for the same magnetic moment (and resulting crustal field) as a thicker layer of a mineral with lower M_s. However, a high T_C can allow a mineral with low M_s to hold a stable remanent magnetization to greater depths, producing a stronger total magnetic moment. Further complication is introduced by the variability of the M_s of a given material with temperature, typically decreasing as temperature increases toward T_C. In the absence of independent constraints on magnetic mineralogy or the magnetizing field, these relationships among magnetic layer thickness, Curie temperature, saturation magnetization, and magnetizing field strength result in nonunique solutions in the modeling of the geophysical properties of Mercury's crust and the evolution of the dynamo field.

3.2. Alteration and Demagnetization of Remanence

Thermal processes are common mechanisms of demagnetization or remagnetization in planetary lithospheres. As a population of ferromagnetic minerals is heated above its T_C subsequent to initial remanence acquisition, any prior statistical alignment of magnetization is progressively erased such that a new

remanence dependent on ambient magnetic field conditions is recorded on cooling. Thermal remagnetization is commonly associated with magmatic systems on Earth and Mars and could also occur on Mercury. However, the geographical variation in surface temperatures related to changes in orbital eccentricity and spin-orbit resonance at Mercury [*Vasavada et al.*, 1999; *Siegler et al.*, 2013] may produce regions in which thermal fluctuations independent of igneous processes contribute to remagnetization.

The chemical alteration of existing minerals can produce a secondary CRM, overprinting part or all of the original remanence. The acquisition of secondary CRM on Earth is commonly the result of oxidation or grain growth through a critical blocking volume, often mediated by fluid movement through the crust. Combinations of modeling and imagery have been used to establish the presence of water ice at shallow depths in Mercury's crust and in its permanently shadowed regions [e.g., *Harmon et al.*, 2011; *Siegler et al.*, 2013; *Vasavada et al.*, 1999]. The role of related fluids in modifying the mineralogy of Mercurian crustal minerals is poorly constrained, but if subsurface fluid motion has occurred during Mercury's evolution, this mechanism has the potential to create localized zones of varied oxidation state.

Shock-induced pressure remanent magnetization (PRM) can play a major role in remagnetization and demagnetization mechanisms. PRM is thought to have been important early in the history of Mars [*Gattacceca et al.*, 2010; *Louzada et al.*, 2011] and may also have contributed to the observed lunar crustal field record [*Wieczorek et al.*, 2012; *Weiss and Tikoo*, 2014], altering the original remanence of crustal materials during impact crater formation. The resulting patterns of magnetization correspond with crater features and are often identifiable from spacecraft orbit [*Louzada et al.*, 2011]. Although the PRM process is typically less efficient than TRM, distinguishing the signatures of these two mechanisms requires additional information about the relative timing, intensity, and types of magnetization in the surrounding terrain.

Viscous remanent magnetization (VRM) is progressively acquired through the realignment of magnetic moments as a material is exposed to a magnetic field different from the field in which it acquired its original remanence. The acquisition rate of a viscous magnetization varies as a function of temperature and grain size, which control the material's relaxation time [*Néel*, 1949; *Pullaiah et al.*, 1975]. Generalized models have been developed to predict the behavior of VRM for common terrestrial minerals like magnetite, hematite, and pyrrhotite [*Pullaiah et al.*, 1975; *Moskowitz*, 1985; *Dunlop et al.*, 2000; *Jackson and Worm*, 2001] and applied to the decay of thermal remanence in Martian crustal systems [*Dunlop and Arkani-Hamed*, 2005]. Additionally, a model for pure iron was developed and applied to lunar crustal magnetizations [*Garrick-Bethell and Weiss*, 2010]. These models give a broad, though useful, approximation of the demagnetizing and remagnetizing effects, as they typically assume that a material is composed exclusively of either single domain grain sizes or multidomain grain sizes, whereas real rocks contain a broad range of grain sizes and shapes.

The behavior of the planetary field may also affect acquisition of VRM. Although Mercury's dynamo field shows no definitive evidence for secular variation over the past 40 years [*Philpott et al.*, 2014], its long-term stability is not yet known. In a dipolar field that undergoes reversals or dramatic changes in intensity, viscous mechanisms would lead to the overall decay of crustal magnetization as new magnetic moments progressively cancel. In contrast, a nonreversing dynamo could result in a progressive increase in bulk magnetization as the extent of moment alignment increases.

3.3. Induced Magnetization

On Earth and Mercury, crustal minerals can acquire an induced magnetization in the planet's modern field. For materials that already hold remanent magnetization, the resulting net magnetization ($\boldsymbol{M}_{\text{net}}$) is a vector sum of two distinct magnetic sources, one modern ($\boldsymbol{M}_{\text{ind}}$) and one ancient ($\boldsymbol{M}_r$):

$$\boldsymbol{M}_{\text{net}} = \boldsymbol{M}_{\text{ind}} + \boldsymbol{M}_r = \kappa \boldsymbol{H}_{\text{modern}} + \boldsymbol{M}_r \tag{1}$$

where κ is the low field susceptibility and $\boldsymbol{H}_{\text{modern}}$ is the present-day applied field [*McEnroe et al.*, 2009]. The material's saturation magnetization gives a theoretical maximum value for $\boldsymbol{M}_{\text{net}}$.

4. Implications for Mercury

Here we address the possible magnetic mineralogy of Mercury, evaluating both previously proposed minerals and several new classes of magnetic minerals with respect to the constraints described above and defining criteria for the assessment of additional materials as potential carriers of remanence.

4.1. Criteria for New Candidate Minerals

A complete determination of the magnetic mineralogy of Mercury is precluded by the limited chemical and geophysical data available. However, according to the constraints described above, candidate magnetic minerals must meet the following criteria:

Low f_{O2}. Oxygen fugacity conditions at Mercury are expected to be highly reducing throughout the planet. For a mineral to be thermodynamically stable in the crust, where magnetic anomalies are expected to originate, its f_{O2} must fall into the reported range of −6.3 to −2.6 ΔIW [*McCubbin et al.*, 2012].

Iron efficient. Compared to the crusts of the Earth and Mars, iron is relatively scarce in that of Mercury, though its geographic distribution is broad [*Dunlop and Arkani-Hamed*, 2005; *Weider et al.*, 2012, 2014]. *Weider et al.* [2014] interpret this distribution to suggest that Fe is primarily contained within iron-poor minerals. However, small volumes of Fe-rich minerals, in particular, configurations (see section 4.2.1) could account for the strong measured remanence.

T_C greater than T_S for remanent magnetization. The minimum required Curie temperature for stable thermal remanence varies regionally with surface temperature conditions, but in all cases, T_C must be greater than T_S at the candidate's source location. The lowest T_C allowed for any candidate is 92 K, the lowest temperature projected at ∼1 m depth in Mercury's crust.

There is no minimum required saturation magnetization for existence at Mercury, but M_s determines the intensity of remanent magnetization that may be recorded, which in turn controls the likelihood of detection of magnetic anomalies from orbit. Candidate minerals must have either a high M_s or a low M_s coupled with a high T_C to produce stronger magnetizations at lower volumes.

4.2. Evaluation of Candidate Minerals

Previous studies of Mercurian magnetism (Table 1) have suggested a range of candidates falling into three categories: iron sulfides, iron silicides, and iron alloys. The list of candidates included here is intentionally broad, including both minerals whose compositions have been proposed to account for the iron detected by orbital spectrometry and minerals whose magnetic properties have been proposed to to be responsible for crustal magnetism on Mercury, including iron-rich paramagnetic and diamagnetic minerals. We address this diverse array of candidates in order to explicate their viability as potential carriers of magnetic remanence with respect to magnetic criteria.

Because of its relatively high f_{O2}, magnetite (Fe_3O_4) is unlikely to be stable on Mercury; it is included here as a point of comparison for less well-studied minerals. Minerals occurring within the ilmenite ($FeTiO_3$)-geikielite ($MgTiO_3$) solid solution series [*Denevi et al.*, 2009; *Lawrence et al.*, 2010; *Riner et al.*, 2010] are unlikely to be present because of their high, narrow f_{O2} stability range [*Ghiorso*, 1990]. They are also not eligible carriers of remanent magnetization due to their very low T_C values, as nowhere on Mercury are conditions cool enough to allow them to act as ferromagnetic carriers.

Iron sulfides have been suggested as candidates for remanence because of the abundance of sulfur in Mercury's crust [*McCubbin et al.*, 2012; *Weider et al.*, 2014; *Johnson et al.*, 2015]. *Johnson et al.* [2015] use pyrrhotite (Fe_7S_8) as a model mineral, but note that its presence is unlikely due to the planet's extremely reducing oxygen fugacity conditions. Although the T_C for pyrrhotite is 320–325°C (∼593–598 K), more than 100°C lower than the maximum daily surface temperature of Mercury, it could retain a TRM at depths greater than those penetrated by the diurnal temperature wave (∼1 m) for the thermal gradients and surface insolation pattern present today. Other iron sulfides suggested as repositories of iron on Mercury have a range of Curie temperatures. Although greigite (Fe_3S_4) has a sufficiently high T_C to be stable in the upper crust, daubréelite ($FeCr_2S_4$), which is found primarily in meteorites [*Kohout et al.*, 2010], would only be able to hold remanence in regions close to the north and south poles where T_S is lowest. Troilite (FeS) may be a thermodynamically stable carrier of iron at Mercury [*Weider et al.*, 2014], but it is not expected to hold magnetic remanence due to its antiferromagnetic character [*Cuda et al.*, 2011]. Additional types of sulfides that can accommodate Fe substitution have been suggested as possible magnetic carriers based on their presence in enstatite chondrite meteorites, including niningerite (MgS) and djerfisherite ($K_6Na(Fe,Cu,Ni)_{25}S2_6Cl$), which is also found in skarns, pegmatites, and kimberlites on Earth [*Anthony et al.*, 2003]. These minerals could be stable under highly reducing conditions like those on Mercury [*Wadhwa*, 2008], although information on their magnetic character is lacking.

Table 1. Magnetic Minerals Previously Suggested to Hold Magnetization or to Contain Fe in Mercury's Crust[a]

Group	Mineral	Formula	T_C (°C)	M_s (Am^2/kg)	Candidate?	Comments
Oxides	Magnetite	Fe_3O_4	575–585[l]	90–92[l]	NO	Unstable due to f_{O2} conditions.
	Ilmenite[b,c,d]	$FeTiO_3$	−233[e,l] (T_N)	0[l,o]	NO	Insufficient Fe and Ti available[f]; low T_N.
	Geikielite[c]	$MgTiO_3$			NO	Unstable due to f_{O2} conditions.
Sulfides	Daubréelite[f]	$FeCr_2S_4$	~−143 – −113[l]	32 at 80 K[s]	YES	Could be stable in low-T_S regions.
	Djerfisherite[f]	$K_6Na(Fe,Cu,Ni)_{25}S_{26}Cl$				Magnetic data lacking.
	Greigite	Fe_3S_4	~333[l]	~25[l]	YES	Stable across T_S range.
	Niningerite[f]	(Mg,Fe,Mn)S				Diamagnetic at RT[j].
	Pyrrhotite[g,h]	Fe_7S_8	320[l]–325[g]	20[l]	NO	Unstable due to f_{O2} conditions.
	Troilite[f,g]	FeS	325[m] (T_N)	0	NO	Antiferromagnetic.
Fe Silicides	Fersilicite[f]	FeSi				Magnetic data lacking.
	Ferdisilicite[f]	$FeSi_2$				Magnetic data lacking.
	Hapkeite[f]	Fe_2Si				Magnetic data lacking.
	Perryite[f]	$(Ni,Fe)_5(SiP)_2$				Magnetic data lacking.
	Suessite*	Fe_3Si	580[u]	137.8 at 6.5 K[v]	YES	T_C in range; stable at low f_{O2}.
Fe Phosphides	Schreibersite*	Fe_3P	432[w]	155.4 at 4 K[x]	YES	T_C in range; stable at low f_{O2}.
Fe Alloys	Awaruite*	Ni_3Fe	620[l]	120[l]	YES	T_C in range; stable at low f_{O2}.
	Tetrataenite*	FeNi	550[l]	130–160[n]	YES	T_C in range; stable at low f_{O2}.
	Wairauite*	CoFe	986[l]	235[l]	YES	T_C in range; stable at low f_{O2}.
Fe Metal	Taenite*	γ–Fe		325–375[t]		Paramagnetic at RT[n].
	Martensite*	α_2–Fe				Transitional phase.
	Kamacite*	α–Fe	218[l]	770[l,t]	YES	T_C in range; stable at low f_{O2}.
Fe Carbide	Cohenite*	Fe_3C	210[p]	140[q,r]	YES	T_C in range; stable at low f_{O2}.

[a] T_C indicates Curie temperature (°C); T_N indicates Néel temperature (°C); M_s indicates saturation magnetization (Am^2/kg); blank space indicates lack of data; "*" indicates new suggestions from this study. Candidacy is assessed here on the basis of temperature and thermodynamic stability alone. Magnetite is not likely to be a candidate mineral, but as its properties are well known, it is included here for comparison to suggested candidates. See main text for additional information.

[b] *Denevi et al.* [2009].
[c] *Riner et al.* [2010].
[d] *Lawrence et al.* [2010].
[e] *Navarrete et al.* [2006]
[f] *Weider et al.* [2014].
[g] *Johnson et al.* [2015].
[h] *Aharonson et al.* [2004].
[i] *Kohout et al.* [2007].
[j] *Farrell et al.* [2002].
[k] *McCubbin et al.* [2012].
[l] *Harrison and Feinberg* [2009].
[m] *Kohout et al.* [2010].
[n] *Gattacceca et al.* [2014].
[o] *Brown et al.* [1993].
[p] *Ivanisenko et al.* [2003].
[q] *Hofer and Cohn* [1959].
[r] *Sajitha et al.* [2007].
[s] *Kohout et al.* [2007].
[t] *Garrick-Bethell and Weiss* [2010].
[u] *Stearns* [1968].
[v] *Hines et al.* [1976].
[w] *Goto et al.* [1977].
[x] *Meyer and Cadeville* [1962].

Iron silicides form under extremely reducing conditions and have been observed in aubrites and lunar samples [e.g., *Anand et al.*, 2004; *Spicuzza et al.*, 2011], suggesting that they may be feasible candidates for iron-bearing minerals on Mercury [*Weider et al.*, 2014]. For instance, both perryite $((Ni,Fe)_5(SiP)_2)$ and the *iron phosphide* schreibersite are found in aubrites [*Weider et al.*, 2014] and in association with kamacite in unequilibrated enstatite chondrites [*Casanova et al.*, 1993; *Rubin*, 1997]. Hapkeite (Fe_2Si) has been identified in association with fersilicite (FeSi) and ferdisilicite ($FeSi_2$) in lunar regolith breccias, consistent with formation in highly reducing lunar soil conditions [*Anthony et al.*, 2003]. These minerals have also been suggested to form through high-temperature shock melting that induces metal-silicate immiscibility [*Spicuzza et al.*, 2011]. However, with the exception of suessite (Fe_3Si), their magnetic properties are not well characterized.

Iron metal and iron alloys are well established as carriers of magnetic remanence in extraterrestrial materials, especially lunar samples and iron meteorites derived from small bodies. Kamacite (α-Fe), martensite (α_2-Fe), and taenite (γ-Fe) are major contributors to remanent magnetization in such materials due to their high saturation magnetization values. In addition, three iron alloys found in meteorites are considered here as candidates, based on their high Curie temperatures: awaruite (Ni_2Fe to Ni_3Fe), tetrataenite (FeNi), and wairauite (CoFe), all of which have $T_C > 500°C$ (~773 K). These minerals are expected to be stable in highly reducing conditions, and both taenite and tetrataenite have previously been found in reduced aubrite meteorites [*Rochette et al.*, 2009]. Nickel has not yet been detected on the surface of Mercury, but this does not preclude the possibility of its presence. Other elements known to form magnetic alloys with iron, including aluminum and titanium, are present in varying amounts [*Nittler et al.*, 2011; *Evans et al.*, 2012]. Iron could also be contained in ferromagnesian silicates [*Riner et al.*, 2010]. The thermal and shock histories of the Mercurian crust may induce precipitation of Fe-Ni inclusions within silicate hosts, as discussed further in section 4.2.1. The phases present in a particular region will depend on its thermal history and cooling rates, which likely vary between regions. In general, for magnetic sources in the deep crust, cooling rates relevant to deep igneous intrusions and slow cooling after impacts will be most relevant (tens of K/Ma). For sources nearer the surface, cooling rates associated with extrusives and shallow intrusives are possible and would result in different phases and microstructures.

Iron carbides are introduced here as possible carriers of magnetic remanence on Mercury because of recent evidence for carbon in Mercury's crust [*Vander Kaaden and McCubbin*, 2015; *Peplowski et al.*, 2016]. Iron carbides with various compositions, including cohenite (Fe_3C) and haxonite ($(Fe,Ni)_{23}C_6$), have been reported in iron meteorites in association with kamacite and taenite [*Rubin*, 1997]. Cohenite, in particular, has been found in basaltic rocks on Earth [e.g., *Goodrich and Bird*, 1985], in aubrite meteorites [*Rochette et al.*, 2009], in lunar samples [*Goldstein et al.*, 1976; *Rochette et al.*, 2010], and as an intermediary phase during diamond formation, consistent with thermodynamic stability in highly reducing conditions [*Palyanov et al.*, 2013]. With a T_C sufficient to hold remanence in the upper crust of Mercury [*Ivanisenko et al.*, 2003] and high saturation magnetization [*Hofer and Cohn*, 1959; *Sajitha et al.*, 2007], iron carbides merit inclusion as candidate minerals.

4.2.1. Additional Considerations: Effects of Grain Size and Microstructures

In spite of the low availability of iron in Mercury's lithosphere relative to the Earth and Mars, iron minerals dominate the list of suggested magnetic remanence carriers. An ideal magnetic mineral would therefore be capable of producing substantial magnetizations while being consistent with petrological constraints on plausible iron and crustal compositions for Mercury. Minerals relevant for remanent magnetization also need to be able to retain their magnetization on billion-year timescales.

Magnetic domain states, which correlate generally with grain size, control magnetic recording behavior in ferromagnetic materials. Single domain grains are most likely to hold stable remanence on geologic timescales, but larger multidomain grains, including those found in some lunar rocks and chondrite meteorites, are possible carriers of remanence due to defects and domain pinning [*Lindquist et al.*, 2015; *Suavet et al.*, 2014; *Gattacceca et al.*, 2014]. Shape anisotropy also affects magnetization, giving rise to increased intensity and stability over isotropic grains. The most stable possible magnetization in an SD grain of a given volume is associated with extreme shape anisotropy, particularly when magnetization is acquired parallel to the long axis of an elongated grain. This relationship holds across magnetic mineralogies: elongate grains of iron are known to be capable of a stable SD size [*Butler and Banerjee*, 1975], while plate-like and pencil-like grains of hematite have demonstrated nearly square hysteresis behavior [*Kletetschka et al.*, 2000].

The distribution of domain states in Mercury's crust (and by extension the grain size distribution of its magnetic minerals) will play an important role in determining the ratio of remanent magnetization to induced magnetization, conventionally referred to as the Koenigsberger ratio, or Q value, and defined as

$$Q = \frac{\boldsymbol{M}_r}{\boldsymbol{M}_{\text{ind}}} = \frac{\boldsymbol{M}_r}{\kappa \boldsymbol{H}_{\text{modern}}}. \quad (2)$$

The susceptibility of MD grains is typically high, as weak fields are capable of driving their domains into configurations whose net magnetizations are in equilibrium with the applied field, while strong fields are required to significantly alter the magnetizations of SD grains, whose low-field susceptibilities are therefore relatively low. As a result, rocks dominated by SD grains will have low induced magnetizations and high Q values, whereas rocks dominated by MD grains will have comparatively stronger induced magnetization and low Q values. An improved understanding of the processes that control the grain size distribution of magnetic minerals on Mercury will ultimately lead to an improved interpretation of the magnetic anomalies observed by MESSENGER by disentangling induced and remanent components of the total measured magnetization.

Magnetic microstructures will also play an important role in the ability of Mercury's crust to retain a permanent remanent magnetization. Such microstructures range from atomic to micrometer length scales and include common mineral phenomena such as atomic vacancies, edge and screw dislocations, stacking faults, inclusions, and intergrowth textures associated with spinodal decomposition and/or exsolution in slowly cooled systems. Iron sulfides, alloys, and oxides commonly exhibit such microstructures, all of which tend to increase the stability of a material's remanent magnetization with respect to changing fields and temperatures [e.g., *Lindquist et al.*, 2015]. Laboratory studies of samples from meteoritic and lunar environments suggest that magnetic microstructures play a crucial role in the retention of remanence in extraterrestrial systems. For instance, the ferromagnetic mineralogy of ordinary chondrites is dominated by Fe-Ni alloys, such as kamacite, taenite, and tetrataenite, present either as single phases in homogeneous grains or as complex microstructures, often defined by submicrometer-scale intergrowth textures whose development depends on both cooling rate (which controls equilibration) and the abundance of other alloying elements in the system [*Gattacceca et al.*, 2014]. Such intergrowths have the effect of subdividing large grains, which would otherwise exhibit multidomain behavior, into assemblages of interacting single domain grains. Additionally, studies of silicate minerals, such as pyroxenes and feldspars, in eucrites and lunar samples have shown that "clouding" of these minerals is due to the presence of submicrometer inclusions of Fe-Ni metals, sulfides, and ilmenite exsolved along microfractures and dislocation networks [*Bell and Mao*, 1973; *Gooley et al.*, 1974; *Sclar and Bauer*, 1975, 1976; *Dymek et al.*, 1976; *Harlow and Klimentidis*, 1980]. Studies of lamellar magnetism in SD and superparamagnetic particles with hematite-ilmenite lamellae demonstrate that the presence of ferrimagnetic contact layers between lamellae, and their hosts can result in strong remanent magnetization with high coercivity [*Harrison and Redfern*, 2001; *McEnroe et al.*, 2002]. Lamellar magnetism has not yet been studied in many of the candidates for magnetic remanence on Mercury and cannot be ruled out as a possible source of remanence.

4.3. Narratives of Magnetization

Mercury's crust has been subject to extensive modification over time by volcanism and impacts. If initial acquisition of remanence occurred in the presence of an ancient field prior to this modification, the magnetic anomalies detectable above the planet's surface should represent the combination of a natural remanent magnetization and additional magnetic components produced by the later alteration of that magnetization, as well as possible contributions from induced magnetization.

TRM is the most likely mechanism of initial remanence acquisition for regions of Mercury's crust exhibiting the strongest magnetization [*Johnson et al.*, 2016]. The long coherence length scale suggests magnetization at depth with minor contributions from near-surface materials that would have been most susceptible to shock. The correlation between the strongest anomalies and associated magnetizations with the smooth plains in and around the Caloris Basin suggest that the 3.7–3.9 Ga surface age of these units is a plausible lower bound for the age of their initial magnetizing event [*Johnson et al.*, 2015], although younger magnetizations from later intrusives are possible, as noted above.

Mercury's active modern field and high impact flux [*Cintala*, 1992] suggest that shock-induced PRM could act as a secondary remanence mechanism rather than resulting in complete demagnetization, allowing crustal

minerals to acquire a new in-field remanence associated with discrete impact events. Current data do not show clear evidence for a global relationship between crater boundaries and magnetization features [*Johnson et al.*, 2015, 2016]. If a formation with an existing remanence, such as a lava flow holding a TRM, is impacted, then the resulting secondary PRM should be detectable as a magnetically anomalous region defined by anomalies with shorter wavelengths, produced by shallow magnetic layers that are readily altered by surface processes. TRM may also act as a local remagnetization mechanism within crater interiors and in association with later magmatism or near volcanic sources.

Because of Mercury's generally high surface temperatures, VRM may have played an important role in modifying any original crustal magnetization [*Johnson et al.*, 2015]. Depending on the short- and long-term behavior of Mercury's magnetic field (e.g., whether it periodically reverses, consistently displays dipolar configurations, and/or varies in intensity over time), VRM acquisition could diminish or amplify the crust's original remanence. However, in most plausible scenarios, VRM is likely to decrease the intensity of a rock's magnetization. Identification of magnetic carriers will allow the calculation of the extent to which a VRM may have decreased the remanence. VRM is also expected to be more easily acquired in regions where surface temperatures approach the Curie temperatures of constituent minerals [*Pullaiah et al.*, 1975; *Jackson and Worm*, 2001].

Spatial variations in magnetization may allow some discrimination among contributions from possible mineralogies. Figures 2 and 3, together with the discussion of the evolution of heat flow over time, suggest that a possible diagnostic for the presence of remanent magnetization carried by low-T_C minerals would be a spatial distribution of magnetization that correlates with the surface insolation proposed by *Aharonson et al.* [2004]. However, even for low-T_C minerals, such a correlation need not be present if the magnetization required to explain the MESSENGER observations can be carried in a thin layer in the upper crust. On Earth, variations in the strength of magnetization that correlate with latitude have been suggested as a possible test for induced contributions to the magnetization [*Maus and Haak*, 2002], although latitudinal variations in the inducing field strength of a factor of ~2 are, in practice, secondary to variations in susceptibility related to heterogeneous types and distributions of magnetic mineralogy.

4.4. Most Likely Carriers of Magnetization

For a proposed carrier of remanence to be plausible, it must be consistent with the mineralogies expected either in relics of Mercury's primary crust or in secondary crust produced by the melting of mantle material. Given the constraints on Mercury's magnetic mineralogy described above, the minerals responsible for observed crustal anomalies are unlikely to be iron sulfides or iron carbides, unless the resulting magnetization was restricted to geographical regions with low average temperature or to upper crustal depths. Oxide minerals are not expected to be present. Further experimental work will be necessary to determine the candidacy of iron silicides, which are poorly characterized in the rock magnetic literature. Thus, of the previously proposed candidates for magnetic remanence carriers, iron metal and iron alloy minerals are the most promising based on current understandings of the Mercurian crustal environment.

Iron metal and alloys are thermodynamically stable in highly reducing f_{O2} conditions like those present at the surface of Mercury. Their high *M*s values would allow them to acquire and retain strong remanence consistent with the anomalies observed by MESSENGER, even in weak applied fields or if other nonmagnetic minerals contain some of the limited iron in Mercury's crust. In addition, the high T_C values of these materials suggest that their acquired remanence would be resistant to thermal demagnetization in the lithosphere. In comparison to other candidate minerals, iron alloys provide the strongest magnetic signal per unit mass (Table 1). The remanent and induced magnetization of iron alloys, particularly iron-nickel alloys, is strongly influenced by exsolution and spinodal decomposition microstructures. In the Mercurian lithosphere, these grains could exist as discrete grains with complex intergrowths of Fe and Ni, or as metallic inclusions in silicate minerals. However, the susceptibility of iron alloys to thermoremanent magnetization is not well characterized, especially as a function of grain size, making it difficult to assess whether iron alloy minerals could account for a remanent magnetization consistent with the observed anomalies. Our ability to assess the plausibility of these scenarios is limited by the lack of physical samples from Mercury. The determination of fundamental magnetic properties for other suggested minerals will enable a more realistic assessment of their candidacy as carriers of magnetic remanence in Mercury's crust.

Acknowledgments
BES received funding from the University of Minnesota Doctoral Dissertation Fellowship Program. CLJ acknowledges support from the Natural Sciences and Engineering Research Council of Canada and the MESSENGER Participating Scientist Program. This work was supported by NASA grant 15-SSW15_2-0129. This is IRM contribution 1603. All data for this paper is cited and referred to in the reference list. We thank two anonymous reviewers for comments that improved the manuscript.

References

Acuña, M. H., et al. (1999), Global distribution of crustal magnetization discovered by the Mars Global Surveyor MAG/ER experiment, *Science*, *284*(5415), 790–793.
Aharonson, O., M. T. Zuber, and S. C. Solomon (2004), Crustal remanence in an internally magnetized non-uniform shell: A possible source for Mercury's magnetic field?, *Earth Planet. Sci. Lett.*, *218*(3–4), 261–268, doi:10.1016/S0012-821X(03)00682-4.
Alexeev, I. I., et al. (2010), Mercury's magnetospheric magnetic field after the first two MESSENGER flybys, *Icarus*, *209*(1), 23–39, doi:10.1016/j.icarus.2010.01.024.
Anand, M., L. A. Taylor, M. A. Nazarov, J. Shu, H.-K. Mao, and R. J. Hemley (2004), Space weathering on airless planetary bodies: Clues from the lunar mineral hapkeite, *Proc. Natl. Acad. Sci. U.S.A.*, *18*, 6847–6851, doi:10.1073/pnas.0401565101.
Anderson, B. J., M. H. Acuña, H. Korth, M. E. Purucker, C. L. Johnson, J. A. Slavin, S. C. Solomon, and R. L. McNutt (2008), The structure of Mercury's magnetic field from MESSENGER's first flyby, *Science*, *321*, 82–85, doi:10.1126/science.1159081.
Anderson, B. J., C. L. Johnson, H. Korth, M. E. Purucker, R. M. Winslow, J. A. Slavin, S. C. Solomon, R. L. McNutt, J. M. Raines, and T. H. Zurbuchen (2011), The global magnetic field of Mercury from MESSENGER orbital observations, *Science*, *333*(6051), 1859–1862, doi:10.1126/science.1211001.
Anthony, J. W., R. A. Bideaux, K. W. Bladh, and M. C. Nichols (2003), Handbook of Mineralogy.
Aubert, J., J. A. Tarduno, and C. L. Johnson (2010), Observations and models of the long-term evolution of Earth's magnetic field, *Space Sci. Rev.*, *155*(1–4), 337–370, doi:10.1007/s11214-010-9684-5.
Bell, P. M., and H. K. Mao (1973), Optical and chemical analysis of iron in Luna 20 plagioclase, *Geochim. Cosmochim. Acta*, *37*, 755–759.
Brown, N. E., A. Navrotsky, G. L. Nord, and S. K. Banerjee (1993), Hematite-ilmenite (Fe_2O_3–$FeTiO_3$) solid solutions: Determinations of Fe-Ti order from magnetic properties, *Am. Mineral.*, *78*(9–10), 941–951.
Butler, F., and K. Banerjee (1975), Single-domain grain size limits for metallic iron, *J. Geophys. Res.*, *80*(2), 252–259, doi:10.1029/JB080i002p00252.
Byrne, P. K., L. R. Ostrach, C. I. Fassett, C. R. Chapman, B. W. Denevi, A. J. Evans, C. Klimczak, M. E. Banks, J. W. Head, and S. C. Solomon (2016), Widespread effusive volcanism on Mercury likely ended by about 3.5 Ga, *Geophys. Res. Lett.*, *43*, 7408–7416, doi:10.1002/2016GL069412.
Casanova, I., K. Keil, and H. E. Newsom (1993), Composition of metal in aubrites: Constraints on core formation, *Geochim. Cosmochim. Acta*, *57*, 675–682, doi:10.1016/0016-7037(93)90377-9.
Cintala, M. J. (1992), Impact-induced thermal effects in the lunar and Mercurian regoliths, *J. Geophys. Res.*, *97*, 947–973, doi:10.1029/93JE01778.
Correia, A. C. M., and J. Laskar (2009), Mercury's capture into the 3/2 spin-orbit resonance including the effect of core-mantle friction, *Icarus*, *201*, 1–11, doi:10.1016/j.icarus.2008.12.034.
Cuda, J., T. Kohout, J. Tucek, J. Haloda, J. Filip, R. Prucek, and R. Zboril (2011), Low-temperature magnetic transition in troilite: A simple marker for highly stoichiometric FeS systems, *J. Geophys. Res.*, *116*(11), 1–9, doi:10.1029/2011JB008232.
Denevi, B. W., et al. (2009), The evolution of Mercury's crust: A global perspective from MESSENGER, *Science*, *324*(5927), 613–618, doi:10.1126/science.1172226.
Denevi, B. W., et al. (2013), The distribution and origin of smooth plains on Mercury, *J. Geophys. Res. Planets*, *118*(5), 891–907, doi:10.1002/jgre.20075.
Dunlop, D. J., and J. Arkani-Hamed (2005), Magnetic minerals in the Martian crust, *J. Geophys. Res.*, *110*(12), 1–11, doi:10.1029/2005JE002404.
Dunlop, D. J., Ö Özdemir, D. A. Clark, and P. W. Schmidt (2000), Time-temperature relations for the remagnetization of pyrrhotite (Fe_7S_8) and their use in estimating paleotemperatures, *Earth Planet. Sci. Lett.*, *176*(1), 107–116, doi:10.1016/S0012-821X(99)00309-X.
Dymek, R. F., A. L. Albee, and A. A. Chodos (1976), Petrology and origin of Boulders #2 and #3, Apollo 17 Station 2, in *Proceedings of the 7th Lunar Science Conference*, vol. 2, pp. 2335–2378, Pergamon Press, Inc., New York, doi:10.1017/CBO9781107415324.004.
Evans, L. G., et al. (2012), Major-element abundances on the surface of Mercury: Results from the MESSENGER Gamma-Ray Spectrometer, *J. Geophys. Res. Planets*, *117*, E00L07, doi:10.1029/2012JE004178.
Farrell, S. P., M. E. Fleet, I. E. Stekhin, A. Kravtsova, A. V. Soldatov, and X. Liu (2002), Evolution of local electronic structure in alabandite and niningerite solid solutions [(Mn, Fe)S, (Mg, Mn)S, (Mg, Fe)S] using sulfur K- and L-edge XANES spectroscopy, *Am. Mineral.*, *87*, 1321–1332.
Frost, D. J., and C. A. McCammon (2008), The redox state of Earth's mantle, *Annu. Rev. Earth Planet. Sci.*, *36*, 389–420, doi:10.1146/annurev.earth.36.031207.124322.
Fuller, M. (1998), Lunar magnetism — A retrospective view of the Apollo sample magnetic studies, *Phys. Chem. Earth*, *23*(7–8), 725–735.
Garrick-Bethell, I., and B. P. Weiss (2010), Kamacite blocking temperatures and applications to lunar magnetism, *Earth Planet. Sci. Lett.*, *294*(1–2), 1–7, doi:10.1016/j.epsl.2010.02.013.
Gattacceca, J., M. Boustie, E. Lima, B. P. Weiss, T. de Resseguier, and J. P. Cuq-Lelandais (2010), Unraveling the simultaneous shock magnetization and demagnetization of rocks, *Phys. Earth Planet. Inter.*, *182*(1–2), 42–49, doi:10.1016/j.pepi.2010.06.009.
Gattacceca, J., C. Suavet, P. Rochette, B. P. Weiss, M. Winklhofer, M. Uehara, and J. M. Friedrich (2014), Metal phases in ordinary chondrites: Magnetic hysteresis properties and implications for thermal history, *Meteorit. Planet. Sci.*, *49*(4), 652–676, doi:10.1111/maps.12268.
Ghiorso, M. S. (1990), Thermodynamic properties of hematite–ilmenite–geikielite solid solutions, *Contrib. to Mineral. Petrol.*, *104*, 645–667, doi:10.1007/BF01167285.
Goldstein, J. I., R. H. Hewins, and A. D. Romig Jr. (1976), Carbides in lunar soils and rocks, in *Proceedings of the 7th Lunar Science Conference*, vol. 1, pp. 807–818, Pergamon Press, Inc., New York.
Goodrich, C. A., and J. M. Bird (1985), Formation of iron-carbon alloys in basaltic magma at Uivfaq, Disko Island: The role of carbon in mafic magmas, *J. Geol.*, *93*(4), 475–492.
Gooley, R., R. Brett, J. Warner, and J. R. Smyth (1974), A lunar rock of deep crustal origin: Sample 76535, *Geochim. Cosmochim. Acta*, *38*, 1329–1339, doi:10.1016/0016-7037(74)90091-X.
Goto, M., H. Tange, T. Tokunaga, H. Fujii, and T. Okamoto (1977), Magnetic properties of the (Fe1-xMx)3P compounds, *Jpn. J. Appl. Phys.*, *16*(12), 2175–2179.
Grott, M., D. Breuer, and M. Laneuville (2011), Thermo-chemical evolution and global contraction of Mercury, *Earth Planet. Sci. Lett.*, *307*(1–2), 135–146, doi:10.1016/j.epsl.2011.04.040.
Harlow, G. E., and R. Klimentidis (1980), Clouding of pyroxene and plagioclase in eucrites: Implications for post-crystallization processing, *Proceedings of the 11th Lunar and Planetary Science Conference*, *2*, 1131–1143, doi:10.1017/CBO9781107415324.004.
Harmon, J. K., M. A. Slade, and M. S. Rice (2011), Radar imagery of Mercury's putative polar ice: 1999–2005 Arecibo results, *Icarus*, *211*, 37–50, doi:10.1016/j.icarus.2010.08.007.
Harrison, R. J., and J. M. Feinberg (2009), Mineral magnetism: Providing new insights into geoscience processes, *Elements*, *5*(4), 209–215, doi:10.2113/gselements.5.4.209.

Harrison, R. J., and S. A. T. Redfern (2001), Short- and long-range ordering in the ilmenite-hematite solid solution, *Phys. Chem. Miner.*, *28*(6), 399–412, doi:10.1007/s002690100167.
Haynes, W. M., T. J. Bruno, and D. R. Lide (2016), *CRC Handbook of Chemistry and Physics*, 96th ed., CRC Press, Boca Raton, Fla.
Head, J. W., et al. (2011), Flood volcanism in the northern high latitudes of Mercury revealed by MESSENGER, *Science*, *333*(6051), 1853–1856, doi:10.1126/science.1211997.
Hines, W. A., A. H. Menotti, J. I. Budnick, T. J. Burch, T. Litrenta, V. Niculescu, and K. Raj (1976), Magnetization studies of binary and ternary alloys based on Fe_3Si, *Phys. Rev. B*, *13*(9), 4060–4068.
Hofer, L., and E. M. Cohn (1959), Saturation magnetizations of iron carbides, *J. Am. Chem. Soc.*, *81*(7), 1576–1582, doi:10.1021/ja01516a016.
Hood, L. L. (2015), Initial mapping of Mercury's crustal magnetic field: Relationship to the Caloris impact basin, *Geophys. Res. Lett.*, *42*, 10,565–10,572, doi:10.1002/2015GL066451.
Hulot, G., T. J. Sabaka, N. Olsen, and A. Fournier (2015), The present and future geomagnetic field, in *Treatise on Geophysics*, 2nd ed., vol. 5, edited by G. Schubert, pp. 33–78, Elsevier, Amsterdam.
Ivanisenko, Y., W. Lojkowski, R. Z. Valiev, and H.-J. Fecht (2003), The mechanism of formation of nanostructure and dissolution of cementite in a pearlitic steel during high pressure torsion, *Acta Mater.*, *51*, 5555–5570, doi:10.1016/S1359-6454(03)00419-1.
Jackson, A., A. R. T. Jonkers, and M. R. Walker (2000), Four centuries of geomagnetic secular variation from historical records, *Philos. Trans. R. Soc. A Math. Phys. Eng. Sci.*, *358*(1768), 957–990, doi:10.1098/rsta.2000.0569.
Jackson, M., and H. U. Worm (2001), Anomalous unblocking temperatures, viscosity and frequency-dependent susceptibility in the chemically-remagnetized Trenton limestone, *Phys. Earth Planet. Inter.*, *126*(1–2), 27–42, doi:10.1016/S0031-9201(01)00242-4.
James, P. B., M. T. Zuber, R. J. Phillips, and S. C. Solomon (2014), Support of long-wavelength topography on Mercury inferred from MESSENGER measurements of gravity and topography, *J. Geophys. Res. Planets*, *120*, 287–310, doi:10.1002/2014JE004713.
Johnson, C. L., et al. (2012), MESSENGER observations of Mercury's magnetic field structure, *J. Geophys. Res. Planets*, *117*(12), 1–22, doi:10.1029/2012JE004217.
Johnson, C. L., et al. (2015), Low-altitude magnetic field measurements by MESSENGER reveal Mercury's ancient crustal field, *Science*, *348*, 892–895.
Johnson, C. L., et al. (2016), *Mercury's crustal magnetic field from low-altitude measurements by MESSENGER*, Lunar Planetary Science, Lunar and Planetary Institute, Houston.
Kletetschka, G., P. J. Wasilewski, and P. T. Taylor (2000), Hematite vs. magnetite as the signature for planetary magnetic anomalies?, *Phys. Earth Planet. Inter.*, *119*(3–4), 259–267, doi:10.1016/S0031-9201(00)00141-2.
Kletetschka, G., P. J. Wasilewski, and P. T. Taylor (2000), Mineralogy of the sources for magnetic anomalies on Mars, *Meteorit. Planet. Sci.*, *35*(5), 895–899, doi:10.1111/j.1945-5100.2000.tb01478.x.
Kohout, T., A. Kosterov, M. Jackson, L. J. Pesonen, G. Kletetschka, and M. Lehtinen (2007), Low-temperature magnetic properties of the Neuschwanstein EL6 meteorite, *Earth Planet. Sci. Lett.*, *261*(1–2), 143–151, doi:10.1016/j.epsl.2007.06.022.
Kohout, T., A. Kosterov, M. Jackson, L. J. Pesonen, G. Kletetschka, and M. Lehtinen (2007), Daubreelite and troilite as a source of cometary and minor body magnetism in cold environment, in *Proceedings of the 70th Annual Meteoritical Society Meeting*, Meteoritics and Planetary Science Supplement, vol. 42, pp. 5209, Tucson, Ariz.
Kohout, T., A. Kosterov, J. Haloda, P. Týcová, and R. Zbořil (2010), Low-temperature magnetic properties of iron-bearing sulfides and their contribution to magnetism of cometary bodies, *Icarus*, *208*(2), 955–962, doi:10.1016/j.icarus.2010.03.021.
Korte, M., C. Constable, F. Donadini, and R. Holme (2011), Reconstructing the Holocene geomagnetic field, *Earth Planet. Sci. Lett.*, *312*(3–4), 497–505, doi:10.1016/j.epsl.2011.10.031.
Lawrence, D. J., W. C. Feldman, J. O. Goldsten, T. J. McCoy, D. T. Blewett, W. V. Boynton, L. G. Evans, L. R. Nittler, E. A. Rhodes, and S. C. Solomon (2010), Identification and measurement of neutron-absorbing elements on Mercury's surface, *Icarus*, *209*(1), 195–209, doi:10.1016/j.icarus.2010.04.005.
Lindquist, A. K., J. M. Feinberg, R. J. Harrison, J. C. Loudon, and A. J. Newell (2015), Domain wall pinning and dislocations: Investigating magnetite deformed under conditions analogous to nature using transmission electron microscopy, *J. Geophys. Res. Solid Earth*, *120*(3), 1415–1430, doi:10.1002/2014JB011335.
Louzada, K. L., S. T. Stewart, B. P. Weiss, J. Gattacceca, R. J. Lillis, and J. S. Halekas (2011), Impact demagnetization of the Martian crust: Current knowledge and future directions, *Earth Planet. Sci. Lett.*, *305*(3–4), 257–269, doi:10.1016/j.epsl.2011.03.013.
Lucey, P. G., G. J. Taylor, and E. Malaret (1995), Abundance and distribution of iron on the Moon, *Science*, *268*(5214), 1150–1153, doi:10.1126/science.268.5214.1150.
Malavergne, V., M. J. Toplis, S. Berthet, and J. Jones (2010), Highly reducing conditions during core formation on Mercury: Implications for internal structure and the origin of a magnetic field, *Icarus*, *206*(1), 199–209, doi:10.1016/j.icarus.2009.09.001.
Maus, S., and V. Haak (2002), Is the long wavelength crustal magnetic field dominated by induced or by remanent magnetisation?, *J. Ind. Geophys. Union*, *6*(1), 1–5.
McCubbin, F. M., M. A. Riner, K. E. Vander Kaaden, and L. K. Burkemper (2012), Is Mercury a volatile-rich planet?, *Geophys. Res. Lett.*, *39*, L09202, doi:10.1029/2012GL051711.
McEnroe, S. A., R. J. Harrison, P. Robinson, and F. Langenhorst (2002), Nanoscale haematite-ilmenite lamellae in massive ilmenite rock: An example of "lamellar magnetism" with implications for planetary magnetic anomalies, *Geophys. J. Int.*, *151*(3), 890–912, doi:10.1046/j.1365-246X.2002.01813.x.
McEnroe, S. A., K. Fabian, P. Robinson, C. Gaina, and L. L. Brown (2009), Crustal magnetism lamellar magnetism and rocks that remember, *Elements*, *5*(4), 241–246, doi:10.2113/gselements.5.4.241.
Meyer, J. P., and M. C. Cadeville (1962), Magnetic properties of iron-phosphorus compounds, *J. Phys. Soc. Jpn*, *17*, 223–225.
Moskowitz, B. M. (1985), Magnetic viscosity, diffusion after-effect, and disaccommodation in natural and synthetic samples, *Geophys. J. R. Astron. Soc.*, *82*, 143–161.
Navarrete, L., J. Dou, D. M. Allen, R. Schad, P. Padmini, P. Kale, and R. K. Pandey (2006), Magnetization and Curie temperature of ilmenite-hematite ceramics, *J. Am. Ceram. Soc.*, *89*(5), 1601–1604, doi:10.1111/j.1551-2916.2006.00953.x.
Néel, L. (1949), Theory of magnetic viscosity of fine grained ferromagnetics with application to baked clays, *Ann. Geophys.*, *5*(99–136).
Ness, N. F., K. W. Behannon, R. P. Lepping, Y. C. Whang, and K. H. Schatten (1974), Magnetic field observations near Mercury: Preliminary results from Mariner 10, *Science*, *185*(4146), 151–160, doi:10.1126/science.185.4146.151.
Nittler, L. R., et al. (2011), The major-element composition of Mercury's surface from MESSENGER X-ray spectrometry, *Science*, *333*(6051), 1847–50, doi:10.1126/science.1211567.
Padovan, S., M. A. Wieczorek, J.-L. Margot, N. Tosi, and S. C. Solomon (2015), Thickness of the crust of Mercury from geoid-to-topography ratios, *Geophys. Res. Lett.*, *42*, 1029–1038, doi:10.1001/2014GL062487.

Palyanov, Y. N., Y. V. Bataleva, A. G. Sokol, Y. M. Borzdov, I. N. Kupriyanov, V. N. Reutsky, and N. V. Sobolev (2013), Mantle-slab interaction and redox mechanism of diamond formation, *Proc. Natl. Acad. Sci. U.S.A.*, *110*(51), 20,408–20,413, doi:10.1073/pnas.1313340110.
Peplowski, P. N., R. L. Klima, D. J. Lawrence, C. M. Ernst, B. W. Denevi, E. A. Frank, J. O. Goldsten, S. L. Murchie, L. R. Nittler, and S. C. Solomon (2016), Remote sensing evidence for an ancient carbon-bearing crust on Mercury, *Nat. Geosci.*, *9*(4), 273–276, doi:10.1038/ngeo2669.
Pepperhoff, W., and M. Acet (2001), *Constitution and Magnetism of Iron and Its Alloys*, Springer, Berlin.
Philpott, L. C., C. L. Johnson, R. M. Winslow, B. J. Anderson, H. Korth, M. E. Purucker, and S. C. Solomon (2014), Constraints on the secular variation of Mercury's magnetic field from the combined analysis of MESSENGER and Mariner 10 data, *Geophys. Res. Lett.*, *41*, 6627–6634, doi:10.1002/2014GL061401.
Pullaiah, G., E. Irving, K. L. Buchan, and D. J. Dunlop (1975), Magnetization changes caused by burial and uplift, *Earth Planet. Sci. Lett.*, *28*, 133–143, doi:10.1016/0012-821X(75)90221-6.
Riner, M. A., F. M. McCubbin, P. G. Lucey, G. Jeffrey Talyor, and J. J. Gillis-Davis (2010), Mercury surface composition: Integrating petrologic modeling and remote sensing data to place constraints on FeO abundance, *Icarus*, *209*(2), 301–313, doi:10.1016/j.icarus.2010.05.018.
Rochette, P., J. Gattacceca, M. Bourot-Denise, G. Consolmagno, L. Folco, T. Kohout, L. Pesonen, and L. Sagnotti (2009), Magnetic classification of stony meteorites: 3. Achondrites, *Meteorit. Planet. Sci.*, *44*(3), 405–427, doi:10.1111/j.1945-5100.2009.tb00741.x.
Rochette, P., J. Gattacceca, A. V. Ivanov, M. A. Nazarov, and N. S. Bezaeva (2010), Magnetic properties of lunar materials: Meteorites, Luna and Apollo returned samples, *Earth and Planet. Sci. Lett.*, *292*, 383–391, doi:10.1016/j.epsl.2010.02.007.
Rubin, A. E. (1997), Mineralogy of meteorite groups, *Meteorit. Planet. Sci.*, *32*, 231–247, doi:10.1111/j.1945-5100.1997.tb01262.x.
Sajitha, E. P., V. Prasad, S. V. Subramanyam, A. K. Mishra, S. Sarkar, and C. Bansal (2007), Size-dependent magnetic properties of iron carbide nanoparticles embedded in a carbon matrix, *J. Phys. Condens. Matter*, *19*(4), 046214, doi:10.1088/0953-8984/19/4/046214.
Schubert, G., D. L. Turcotte, and P. Olson (2005), *Mantle Convection in the Earth and Planets*, Cambridge Univ. Press, New York.
Sclar, C. B., and J. F. Bauer (1975), Shock-induced subsolidus reduction-decomposition of orthopyroxene and shock-induced melting in norite 78235, in *Proceedings of the 6th Lunar Science Conference*, pp. 799–820, Pergamon Press, Inc., New York, doi:10.1017/CBO9781107415324.004.
Sclar, C. B., and J. F. Bauer (1976), Redox reactions involving nonvolatile ionic species as a mechanism of shock-induced subsolidus reduction of Fe+2 in plagioclase and orthopyroxene: Indications from lunar norite 78235 (abs.), in *Lunar Sci. VII*, pp. 791–793, Lunar and Planetary Institute, Houston, doi:10.1017/CBO9781107415324.004.
Siegler, M. A., B. G. Bills, and D. A. Paige (2013), Orbital eccentricity driven temperature variation at Mercury's poles, *J. Geophys. Res. Planets*, *118*(5), 930–937, doi:10.1002/jgre.20070.
Spicuzza, M. J., J. W. Valley, J. Fournelle, J. M. Huberty, and A. Treiman (2011), Native silicon and Fe-silicides from the Apollo 16 lunar regolith: Extreme reduction, metal-silicate immiscibility, and shock melting, in *Proceedings of the 42nd Lunar and Planetary Science Conference*, 2231 pp.,The Woodlands, Houston, Tex.
Stearns, M. B. (1968), Internal-field variations with temperature for the two sublattices of ordered Fe_3Al and Fe_3Si, *Phys. Rev.*, *168*(2), 588–592.
Suavet, C., B. P. Weiss, and T. L. Grove (2014), Controlled-atmosphere thermal demagnetization and paleointensity analyses of extraterrestrial rocks, *Geochem. Geophys. Geosyst.*, *15*, 2733–2743, doi:10.1002/2013GC005215.
Tikoo, S. M., B. P. Weiss, J. Buz, E. A. Lima, E. K. Shea, G. Melo, and T. L. Grove (2012), Magnetic fidelity of lunar samples and implications for an ancient core dynamo, *Earth Planet. Sci. Lett.*, *337–338*, 93–103, doi:10.1016/j.epsl.2012.05.024.
Tikoo, S. M., B. P. Weiss, W. S. Cassata, D. L. Shuster, J. Gattacceca, E. A. Lima, C. Suavet, F. Nimmo, and M. D. Fuller (2014), Decline of the lunar core dynamo, *Earth Planet. Sci. Lett.*, *404*, 89–97, doi:10.1016/j.epsl.2014.07.010.
Tosi, N., M. Grott, A. C. Plesa, and D. Breuer (2013), Thermochemical evolution of Mercury's interior, *J. Geophys. Res. Planets*, *118*(12), 2474–2487, doi:10.1002/jgre.20168.
Vander Kaaden, K. E., and F. M. McCubbin (2015), Exotic crustal formation on Mercury: Consequences of a shallow, FeO-poor mantle, *J. Geophys. Res. Planets*, *120*, 195–209, doi:10.1002/2014JE004733.
Vasavada, A. R., D. A. Paige, and S. E. Wood (1999), Near-surface temperatures on Mercury and the Moon and the stability of polar ice deposits, *Icarus*, *141*(2), 179–193, doi:10.1006/icar.1999.6175.
Wadhwa, M. (2008), Redox conditions on small bodies, the Moon and Mars, *Rev. Mineral. Geochem.*, *68*(1), 493–510, doi:10.2138/rmg.2008.68.17.
Weider, S. Z., L. R. Nittler, R. D. Starr, T. J. McCoy, K. R. Stockstill-Cahill, P. K. Byrne, B. W. Denevi, J. W. Head, and S. C. Solomon (2012), Chemical heterogeneity on Mercury's surface revealed by the MESSENGER X-Ray Spectrometer, *J. Geophys. Res. Planets*, *117*, E00L05, doi:10.1029/2012JE004153.
Weider, S. Z., L. R. Nittler, R. D. Starr, T. J. McCoy, and S. C. Solomon (2014), Variations in the abundance of iron on Mercury's surface from MESSENGER X-Ray Spectrometer observations, *Icarus*, *235*, 170–186, doi:10.1016/j.icarus.2014.03.002.
Weiss, B. P., and S. M. Tikoo (2014), The lunar dynamo, *Science*, *346*, 6214, doi:10.1126/science.1246753.
Wieczorek, M. A., B. P. Weiss, and S. T. Stewart (2012), An impactor origin for lunar magnetic anomalies, *Science*, *335*, 1212–1216.
Williams, J. P., O. Aharonson, and F. Nimmo (2007), Powering Mercury's dynamo, *Geophys. Res. Lett.*, *34*(21), 2–6, doi:10.1029/2007GL031164.